



Discovery and biological evaluation of some (1*H*-1,2,3-triazol-4-yl) methoxybenzaldehyde derivatives containing an anthraquinone moiety as potent xanthine oxidase inhibitors



Ting-jian Zhang, Song-ye Li¹, Wei-yan Yuan¹, Qing-xia Wu, Lin Wang, Su Yang, Qi Sun, Fan-hao Meng*

School of Pharmacy, China Medical University, 77 Puhe Road, North New Area, Shenyang 110122, China

ARTICLE INFO

Article history:

Received 14 September 2016

Revised 28 December 2016

Accepted 14 January 2017

Available online 16 January 2017

Keywords:

Anthraquinone
Xanthine oxidase
Hyperuricemia

ABSTRACT

A series of (1*H*-1,2,3-triazol-4-yl)methoxybenzaldehyde derivatives containing an anthraquinone moiety were synthesized and identified as novel xanthine oxidase inhibitors. Among them, the most promising compounds **1h** and **1k** were obtained with IC₅₀ values of 0.6 μM and 0.8 μM, respectively, which were more than 10-fold potent compared with allopurinol. The Lineweaver-Burk plot revealed that compound **1h** acted as a mixed-type xanthine oxidase inhibitor. SAR analysis showed that the benzaldehyde moiety played a more important role than the anthraquinone moiety for inhibition potency. The basis of significant inhibition of xanthine oxidase by **1h** was rationalized by molecular modeling studies.

© 2017 Elsevier Ltd. All rights reserved.

Xanthine oxidase (XO) is a well-known target for the treatment of hyperuricemia and gout. Inhibition of XO could block the hydroxylation of both hypoxanthine and xanthine in the last two steps of uric acid biosynthesis in humans.¹ Indeed, the over-production of uric acid is the key cause of hyperuricemia and gout.² Therefore, inhibitors of XO could decrease the generation of uric acid and benefit these pathological conditions.³ Reactive oxygen species (ROS) are generated in concert with the oxidation process. An excess of ROS could induce various pathological states such as inflammation, metabolic disorders, atherosclerosis, cancer and chronic obstructive pulmonary disease.⁴ Thus, inhibition of XO is a potential treatment of diseases caused by the XO-derived ROS as well.⁵

Reported XO inhibitors can be simply divided into two categories: purine analogs and non-purine XO inhibitors. Allopurinol (Fig. 1), a prototypical inhibitor of XO with a recognizable purine backbone, has been widely prescribed in the treatment of hyperuricemia and gout for several decades. However, in some cases, severe life-threatening side effects of allopurinol have been reported due to the purine backbone, such as fulminant hepatitis, renal failure, and Stevens–Johnson syndrome.⁶ Given these limitations, research has focused on the development of novel non-purine XO inhibitors with potent XO inhibitory potency, but with

fewer side effects. In recent decades, a great amount of non-purine XO inhibitors of various chemotypes have been reported, such as Febuxostat (approved in USA, 2009),⁷ Y-700,⁸ Topiroxostat (approved in Japan, 2013),⁹ isoxazoles,¹⁰ schiff bases of benzaldehydes,¹¹ *N*-(1,3-diaryl-3-oxo-propyl)amides,¹² *N*-acetyl pyrazolines,¹³ isocytosines,¹⁴ selenazoles,¹⁵ imidazoles,¹⁶ 2-(indol-5-yl)thiazoles,¹⁷ chalcones,¹⁸ and 9-deazaguanines.¹⁹

In our previous studies on anthraquinone compounds as anti-tumor agents, we unexpectedly found a compound (**1a**), which contained a benzaldehyde moiety and an anthraquinone moiety linked by a 1,2,3-triazole (Fig. 1), presented poor anti-tumor activity, but remarkable inhibitory potency *in vitro* against XO. Since both benzaldehyde and anthraquinone have appeared as scaffolds of XO inhibitors in recent studies,²⁰ we investigated the activities and the structure–activity relationship (SAR) around **1a**.

The synthesis of compounds **1a–q** is shown in the Scheme 1. Commercially available phthalic anhydride reacted with toluene via a Friedel–Craft reaction to provide 2-(4-methylbenzoyl)benzoic acid **2**, which underwent an intramolecular cyclization in acid-catalyzed conditions, leading to 2-methylanthracene-9,10-dione **3**. The bromination of **3** with NBS obtained 2-(bromomethyl)anthracene-9,10-dione **4**, which was then treated with sodium azide to yield 2-(azidomethyl)anthracene-9,10-dione **5**. The cyclization of **5** with various alkyne analogs in the presence of copper sulfate and vitamin C in a microwave condition resulted in compounds **1a–o** with good yields. Hydrolysis of compound **1o** with sodium hydroxide resulted in **1p**, which was acetylated to yield **1q**. The

* Corresponding author.

E-mail address: fhmeng@cmu.edu.cn (F.-h. Meng).

¹ These authors contributed equally.

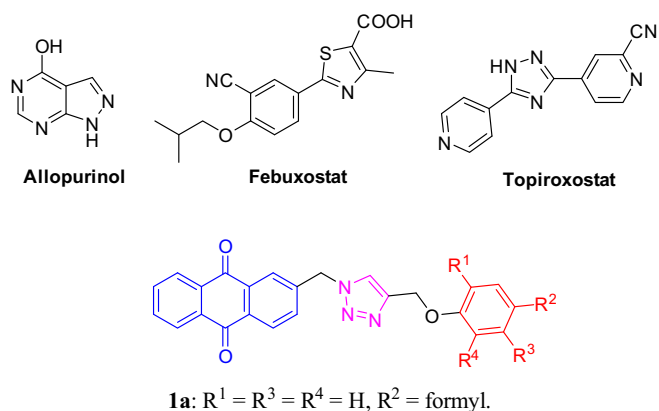


Fig. 1. Chemical structures of Allopurinol, Febuxostat, Topiroxostat and compound **1a**.

structures of the synthesized compounds were elucidated by ¹H NMR, ¹³C NMR, and MS. All spectral data were in accordance with assumed structures.

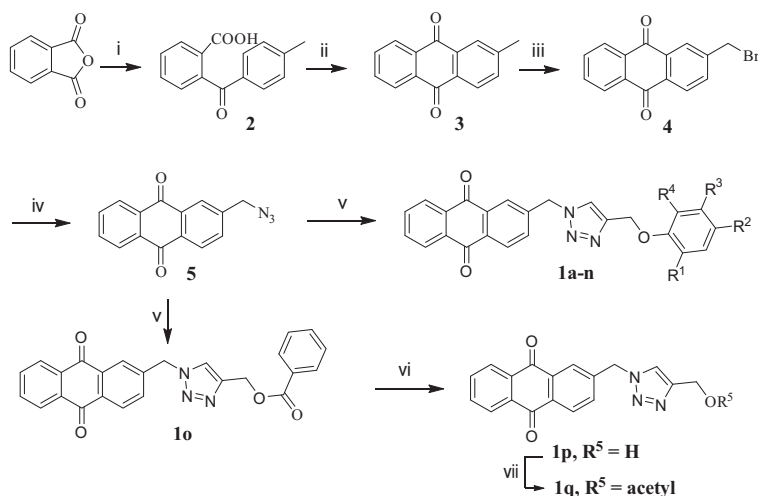
Bovine XO inhibitory potencies *in vitro* were spectrophotometrically measured by determining the uric acid levels at 294 nm. The

testing method has been described in our previous study.¹⁶ Allopurinol was included as a reference compound. Compounds presenting inhibitory effects higher than 60% at the concentration of 50 μM were further tested at a wide range of concentrations to calculate associated IC₅₀ values. The results are shown in Table 1.

Compound **1a** was initially discovered as a weak XO inhibitor (IC₅₀ = 30.5 μM), which was 3-fold less potent than allopurinol (IC₅₀ = 9.8 μM). Removing the phenyl group led to inactive compounds **1p** and **1q**, which implied that the phenyl group may strongly affect the XO inhibitory activity. Therefore, structure-modification efforts to enhance the inhibitory potency were mainly focused on this phenyl group.

The preliminary structure–activity relationship (SAR) around **1a** indicated that the formyl group played a significant role for XO inhibition in this series, in spite of its lower drug-like features. Removal of the formyl group resulted in **1b** and its analog **1c**, accompanied by a decrease of potency. Furthermore, when the *para*-formyl group was changed into a cyano (**1e**) or an acetylamino (**1f**) group, the activities of both were diminished, as well. However, the introduction of two methoxy groups into the *ortho*-position of phenyl ether (**1d**, IC₅₀ = 16.8 μM) led to a 1.8-fold increase in potency.

As shown in Table 1, the position of the formyl group noticeably affected the inhibitory potency. When the *para*-formyl group of **1a**



Scheme 1. Synthesis of compounds **1a–q**. Reagents and conditions: (i) toluene, AlCl₃, 50 °C, 4 h; (ii) H₂SO₄, 100 °C, 1 h; (iii) NBS, CCl₄, reflux, 24 h; (iv) NaN₃, THF, 40 °C, overnight; (v) alkyne derivatives, CuSO₄, vitamin C, EtOH, H₂O, 80 °C, microwave 10 min; (vi) NaOH, MeOH, H₂O, 50 °C, 1.5 h; (vii) acetyl chloride, Et₃N, dichloromethane, 0 °C then 25 °C, 1 h.

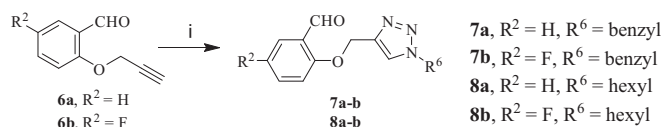
Table 1
XO *in vitro* inhibitory potencies of compounds **1a–q**.

Compounds	R ¹	R ²	R ³	R ⁴	Inhibition rate at 50 μM	IC ₅₀ (μM)
1a	H	Formyl	H	H	67.5	30.5
1b	H	H	H	H	18.4	/
1c	Cl	H	H	Cl	12.7	/
1d	OCH ₃	Formyl	H	OCH ₃	70.3	16.8
1e	H	CN	H	H	7.0	/
1f	H	Acetylamino	H	H	20.1	/
1g	H	H	Formyl	H	77.2	15.1
1h	Formyl	H	H	H	90.7	0.6
1i	Carboxyl	H	H	H	24.2	/
1j	Formyl	H	N(C ₂ H ₅) ₂	H	9.8	/
1k	Formyl	F	H	H	88.0	0.8
1l	Formyl	Cl	H	H	61.1	46.5
1m	Formyl	Br	H	H	21.1	/
1n	Formyl	H	F	H	70.8	6.5
1p	/	/	/	/	31.0	/
1q	/	/	/	/	19.4	/
Allopurinol	/	/	/	/	95.1	9.8

was transferred to the *meta*-position (**1g**, $IC_{50} = 15.1 \mu\text{M}$), the potency was doubled. Moreover, the transition of the formyl group to the *ortho*-position produced the most promising compound **1h** ($IC_{50} = 0.6 \mu\text{M}$), which was 51 times more potent than **1a**.

The following modifications based on **1h** were mainly carried out by introduction of several substituents onto the phenyl unit, such as halogens and *N,N*-diethylamino. Unfortunately, most of the obtained compounds resulted either in a steep loss in potency (**1i**, $IC_{50} = 46.5 \mu\text{M}$ and **1n**, $IC_{50} = 6.5 \mu\text{M}$) or were entirely inactive (**1j** and **1m**). The exception was **1k** ($IC_{50} = 0.8 \mu\text{M}$), possessing a fluorine atom for R_2 , which displayed comparable potency to compound **1h**. In addition, formyl oxidation to carboxyl (**1i**) also diminished the potency. Therefore, the only modification that could maintain the potency was achieved by introducing a fluorine atom for R_2 group in this series, *i.e.*, **1k**.

To investigate the function of the anthraquinone moiety, **1h** analogs with the anthraquinone moiety replaced by a benzyl group or a hexyl group were synthesized (Scheme 2) and evaluated for potency against XO (Table 2). Surprisingly, some of these compounds were also active, such as **7b** ($IC_{50} = 21.5 \mu\text{M}$) and **8b**



Scheme 2. Synthesis of compounds **7a-b** and **8a-b**. Reagents and conditions: (i) (azidomethyl)benzene or azidohexane, CuSO_4 , vitamin C, EtOH, H_2O , 80°C , microwave 10 min.

($IC_{50} = 9.0 \mu\text{M}$), although there was nearly a 10-fold loss in potency compared with **1h**. For the R^6 group, the broad structural tolerance implied that the anthraquinone moiety may act as a supporting role in inhibition of XO. Because the XO binding pocket presents as a long, narrow cavity leading toward the molybdenum-pterin center,⁷ it was concluded that the anthraquinone moiety may be located at the outer region of active pocket, as in the case of the isobutoxy group of Febuxostat, which possessed more tolerance for the structure of the ligands. This hypothesis was confirmed by molecular simulation studies.

To further understand the binding mode of the synthesized compounds, molecular simulations of **1h** into the binding pocket of XO were performed. As the molybdenum-pterin sites of XO and xanthine oxidoreductase are structurally equivalent,²¹ the crystal structure of xanthine oxidoreductase/Febuxostat complex (PDB code 1N5X) was employed as the protein template. A molecular docking study was undertaken with AutoDock 4²² with the default settings. The Lamarckian genetic algorithm was used as the search parameters. MOE (Molecular Operating Environment, version 2015.1001) software was used for graphic display (Fig. 2). According to this model, the benzaldehyde moiety inserted into the long-narrow cavity of the binding pocket and partially overlapped with phenyl moiety of Febuxostat. Additionally, the formyl group accepted a hydrogen bond from the hydroxyl of Ser876. Moreover, the anthraquinone moiety occupied a sub-pocket formed by Phe1013, Leu1014, Ser1075, Lys771 and Met770 outside the cavity, and an H-bond interaction between a carbonyl of anthraquinone and the amino of Lys771 was observed. These interactions may provide a reasonable explanation for the SAR results in the study.

Table 2
XO *in vitro* inhibitory potencies of **1h** analogs.

Compounds	R^2	R^6	Inhibition rate at $50 \mu\text{M}$	IC_{50} (μM)
7a	H	Benzyl	46.7	/
7b	F	Benzyl	83.4	21.5
8a	H	Hexyl	43.5	/
8b	F	Hexyl	93.0	9.0

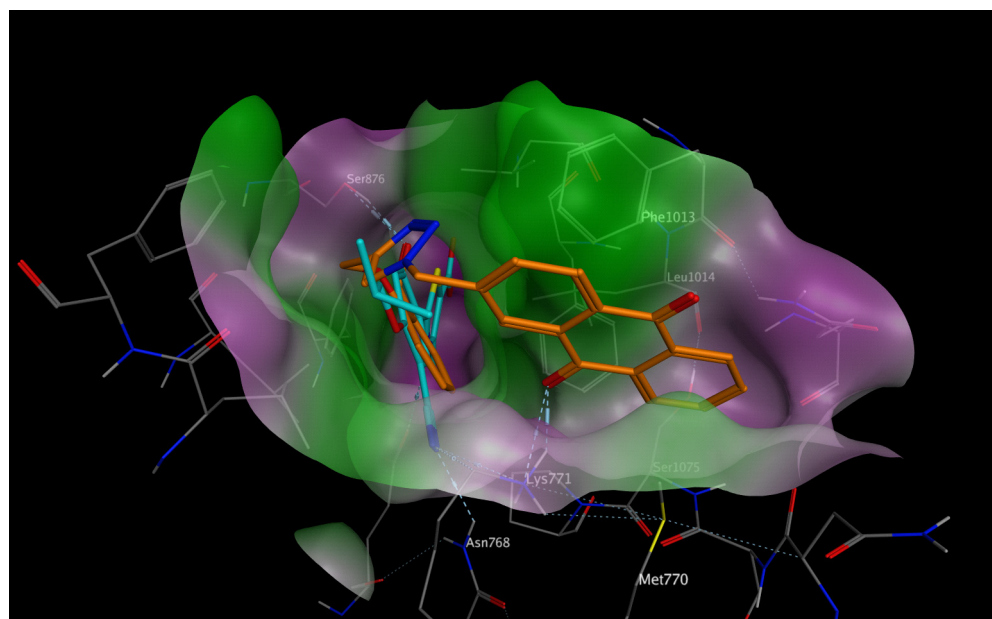


Fig. 2. Docking pose of compound **1h** (orange) within the protein binding pocket overlaid with the reference ligand Febuxostat (cyan).

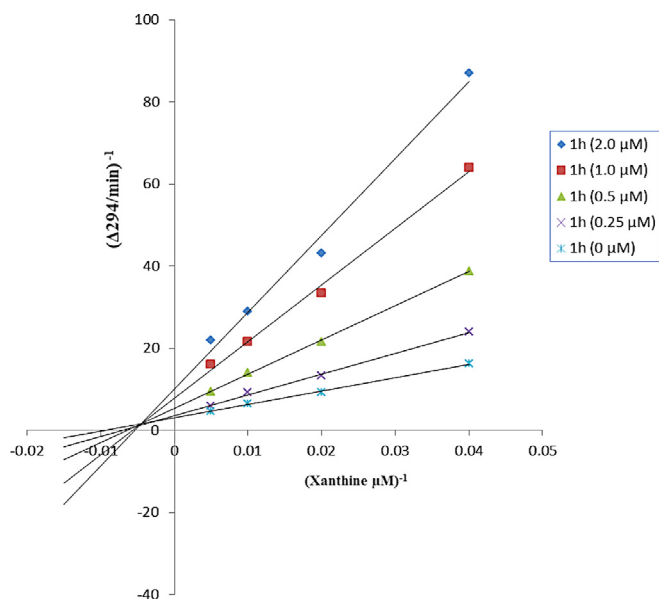


Fig. 3. Lineweaver-Burk plot analysis of xanthine oxidase by compound **1h**.

Steady-state kinetic analysis was performed for representative compound **1h** using the method reported by Matsumoto et al.⁹ The Lineweaver-Burk plot (Fig. 3) revealed that compound **1h** acted as a mixed-type inhibitor on XO. This inhibition type could be explained by potent inhibition of both the oxidized and reduced forms of XO.²³ Similar action was reported with two other inhibitors, Febuxostat⁷ and Y-700.⁸ A K_i value of 0.57 μM was calculated from a secondary plot of the slope from the primary plot versus the inhibitor concentrations and a K_i' value of 0.94 μM was calculated from a plot of the $1/V_{\text{max}}$ versus the inhibitor concentrations.

In summary, (1*H*-1,2,3-triazol-4-yl)methoxybenzaldehyde derivatives containing an anthraquinone moiety were synthesized and identified as novel XO inhibitors. Among them, the most promising compounds **1h** (IC_{50} = 0.6 μM) and **1k** (IC_{50} = 0.8 μM) were obtained and presented more than 10-fold greater potencies than the reference XO inhibitor allopurinol. SAR analysis revealed that the benzaldehyde moiety played a more important role than the anthraquinone moiety in the inhibitory potency. Additionally, a formyl group fixed at the 2-position of phenyl was essential for bioactivity. The Lineweaver-Burk plot showed that compound **1h** acted as a mixed-type XO inhibitor. Molecular modeling provided a reasonable explanation for the structure–activity relationships observed in this study.

Acknowledgments

This work was supported by the Chinese National Science Foundation (Grant Nos. 81274182, 81573687) and the project of Liaoning distinguished professor.

Supplementary material

Supplementary data associated with this article can be found, in the online version, at <http://dx.doi.org/10.1016/j.bmcl.2017.01.049>. These data include MOL files and InChIKeys of the most important compounds described in this article.

References

- Choi HK, Mount DB, Reginato AM. Pathogenesis of gout. *Ann Intern Med.* 2005;143:499.
- Gliozzi M, Malara N, Muscoli S, Mollace V. The treatment of hyperuricemia. *Int J Cardiol.* 2016;213:23.
- Chen C, Lü J-M, Yao Q. Hyperuricemia-related diseases and xanthine oxidoreductase (XOR) inhibitors: an overview. *Med Sci Monitor.* 2016;22:2501.
- Evenäs J, Edfeldt F, Lepistö M, et al. HTS followed by NMR based counterscreening. Discovery and optimization of pyrimidones as reversible and competitive inhibitors of xanthine oxidase. *Bioorg Med Chem Lett.* 2014;24:1315.
- (a) Singh H, Sharma S, Ojha R, Gupta MK, Nepali K, Bedi PMS. Synthesis and evaluation of naphthoflavones as a new class of non purine xanthine oxidase inhibitors. *Bioorg Med Chem Lett.* 2014;24:4192;
(b) Smelcerovic Z, Veljkovic A, Kocic G, et al. Xanthine oxidase inhibitory properties and anti-inflammatory activity of 2-amino-5-alkylidene-thiazol-4-ones. *Chem-Biol Interact.* 2015;229:73.
- Pacher P. Therapeutic effects of xanthine oxidase inhibitors: renaissance half a century after the discovery of allopurinol. *Pharmacol Rev.* 2006;58:87.
- Okamoto K, Eger BT, Nishino T, Kondo S, Pai EF. An extremely potent inhibitor of xanthine oxidoreductase: crystal structure of the enzyme-inhibitor complex and mechanism of inhibition. *J Biol Chem.* 2002;278:1848.
- Ishibuchi S, Morimoto H, Oe T, et al. Synthesis and structure–activity relationships of 1-Phenylpyrazoles as xanthine oxidase inhibitors. *Bioorg Med Chem Lett.* 2001;11:879.
- Matsumoto K, Okamoto K, Ashizawa N, Nishino T. FYX-051: A novel and potent hybrid-type inhibitor of xanthine oxidoreductase. *J Pharmacol Exp Ther.* 2010;336:95.
- Wang S, Yan J, Wang J, et al. Synthesis of some 5-phenylisoxazole-3-carboxylic acid derivatives as potent xanthine oxidase inhibitors. *Eur J Med Chem.* 2010;45:2663.
- Leigh M, Raines DJ, Castillo CE, Duhme-Klair AK. Inhibition of xanthine oxidase by thiosemicarbazones, hydrazones and dithiocarbazates derived from hydroxy-substituted benzaldehydes. *ChemMedChem.* 2011;6:1107.
- Nepali K, Agarwal A, Sapra S, et al. N-(1,3-Diaryl-3-oxopropyl)amides as a new template for xanthine oxidase inhibitors. *Bioorg Med Chem.* 2011;19:5569.
- Nepali K, Singh G, Turan A, et al. A rational approach for the design and synthesis of 1-acetyl-3,5-diaryl-4,5-dihydro(1*H*)pyrazoles as a new class of potential non-purine xanthine oxidase inhibitors. *Bioorg Med Chem.* 2011;19:1950.
- (a) Khanna S, Burudkar S, Bajaj K, et al. Isocytosine-based inhibitors of xanthine oxidase: design, synthesis, SAR, PK and in vivo efficacy in rat model of hyperuricemia. *Bioorg Med Chem Lett.* 2012;22:7543;
(b) Bajaj K, Burudkar S, Shah P, et al. Lead optimization of isocytosine-derived xanthine oxidase inhibitors. *Bioorg Med Chem Lett.* 2013;23:834.
- Guan Q, Cheng Z, Ma X, et al. Synthesis and bioevaluation of 2-phenyl-4-methyl-1,3-selenazole-5-carboxylic acids as potent xanthine oxidase inhibitors. *Eur J Med Chem.* 2014;85:508.
- Chen S, Zhang T, Wang J, et al. Synthesis and evaluation of 1-hydroxy/methoxy-4-methyl-2-phenyl-1*H*-imidazole-5-carboxylic acid derivatives as non-purine xanthine oxidase inhibitors. *Eur J Med Chem.* 2015;103:343.
- Song JU, Choi SP, Kim TH, et al. Design and synthesis of novel 2-(indol-5-yl)thiazole derivatives as xanthine oxidase inhibitors. *Bioorg Med Chem Lett.* 2015;25:1254.
- Hofmann E, Webster J, Do T, et al. Hydroxylated chalcones with dual properties: xanthine oxidase inhibitors and radical scavengers. *Bioorg Med Chem.* 2016;24:578.
- Rodrigues MV, Barbosa AF, da Silva JF, et al. 9-Benzoyl 9-deazaguanines as potent xanthine oxidase inhibitors. *Bioorg Med Chem.* 2016;24:226.
- (a) Lü J-M, Yao Q, Chen C. 3,4-Dihydroxy-5-nitrobenzaldehyde (DHNb) is a potent inhibitor of xanthine oxidase: A potential therapeutic agent for treatment of hyperuricemia and gout. *Biochem Pharmacol.* 2013;86:1328;
(b) Shi D-H, Huang W, Li C, Liu Y-W, Wang S-F. Design, synthesis and molecular modeling of aloe-emodin derivatives as potent xanthine oxidase inhibitors. *Eur J Med Chem.* 2014;75:289.
- Cristofer E, Bryan TE, Ken O, Tomoko N, Takeshi N, Emil FP. Crystal structures of bovine milk xanthine dehydrogenase and xanthine oxidase: Structure-based mechanism of conversion. *PNAS.* 2000;97:10723.
- Morris GM, Huey R, Lindstrom W, et al. AutoDock4 and AutoDockTools4: automated docking with selective receptor flexibility. *J Comput Chem.* 2009;30:2785.
- Okamoto K, Nishino T. Mechanism of inhibition of xanthine oxidase with a new tight binding inhibitor. *J Biol Chem.* 1995;270:7816.